



# The Evolution of the Nucleus Surface in the Context of the Change in the Brightness of a Comet\*

Marcin Wesołowski 

College of Natural Sciences, Institute of Physics, University of Rzeszów, Pigońia 1 Street, 35-310 Rzeszów, Poland; [mwesolowski@ur.edu.pl](mailto:mwesolowski@ur.edu.pl)  
Received 2021 December 31; revised 2022 March 2; accepted 2022 March 21; published 2022 April 29

## Abstract

The paper presents a model of the thermodynamic evolution of the comet nucleus surface. In the proposed approach, we focus on the analysis of the formation of pits visible on the surface of the cometary nucleus. These pits are a consequence of the thermodynamic evolution of both the surface layers and the inner layers of the cometary nucleus. As a result of complex thermodynamic processes, the surface layer is destroyed. A measure of this destruction is the amount of comet material that is thrown into a coma as a result of sublimation. The effect of this process is an increase in the area on which the incident light scatters. Then we can notice a sudden increase in the brightness of the comet, i.e., its outburst. A measure of the amplitude of a given outburst is the diameter and thickness of the surface layer that has been destroyed. The mechanism of the evolution of the pits was proposed based on the analysis of many photos taken by the Rosetta probe. The obtained numerical values correspond to the actual brightness changes of the Jupiter family comets during their outburst.

*Key words:* comets – comet nuclei – comet surfaces

## 1. Introduction

Comets are small celestial bodies that formed during the formation of the solar system. In other words, we can treat comets as cosmic time capsules that contain in their structure a record of the formation of our planetary system. Note that the comets have survived to modern times in a practically unchanged structure. Therefore, studying the properties of cometary nuclei provides me with more and more information about the formation and evolution of the solar system.

The main component of any comet is its nucleus, which is also the carrier of the cometary bulk mass. Comet nuclei are dust conglomerates that contain admixtures of icy material. Analyzing the results of cometary missions, we can see that the dimensions of the dust particles forming the dust agglomerates range from  $10^{-2}$   $\mu\text{m}$  to several centimeters (Güttler et al. 2019). However, most particles that occur in a coma have dimensions comparable to the wavelength of the incident sunlight. Note that organic matter should be classified as dust that has refractory properties at heliocentric distances greater than 1 au. It should be clearly emphasized here that cometary nuclei differ in terms of their chemical composition. The main difference is the percentage of each chemical relative to the water ice. The results regarding the detailed chemical composition of comets were recently summarized in Keller & Kühr (2020). Also, the size of the nucleus and the location in the solar system play important roles.

One of the most interesting manifestations of cometary activity is rapid changes in the brightness of these celestial bodies, i.e., a cometary outburst. When we talk about a cometary outburst, we mean an increase in its brightness usually by several magnitudes (Cabot et al. 1996; Enzian et al. 1997; Ivanova et al. 2011; Gronkowski & Wesołowski 2012, 2015a, 2016; Miles 2016; Wesołowski & Gronkowski 2018a; Wesołowski 2020b, 2021b, 2021c, 2022; Wesołowski et al. 2020b, 2020c). We can present the course of a cometary outburst based on four stages: quiet phase (before the outburst), the outburst phase and the phase after the outburst, achieving a brightness comparable to the pre-outburst phase (see Wesołowski 2021a). In the quiet sublimation phase, the comet looks like a diffuse cloud with central compaction—its nucleus. As a result of an outburst, the coma significantly increases in size compared to the pre-outburst phase. Analyzing the extensive observation material and taking into account the above four phases of the comet blast scenario, we conclude that the entire process takes about several dozen days (Wesołowski 2021d). However, it should be clearly emphasized that the duration of a cometary outburst depends on the amplitude of its brightness.

It should be clearly emphasized that the purpose of this manuscript is not to criticize previous scientific achievements and individual models of a cometary outburst. The approach presented in the paper should be treated as an attempt to develop a new numerical model of a cometary outburst based on the thermodynamic evolution of the surface and subsurface layers of the cometary nucleus.

---

\* University of Rzeszów, Poland.

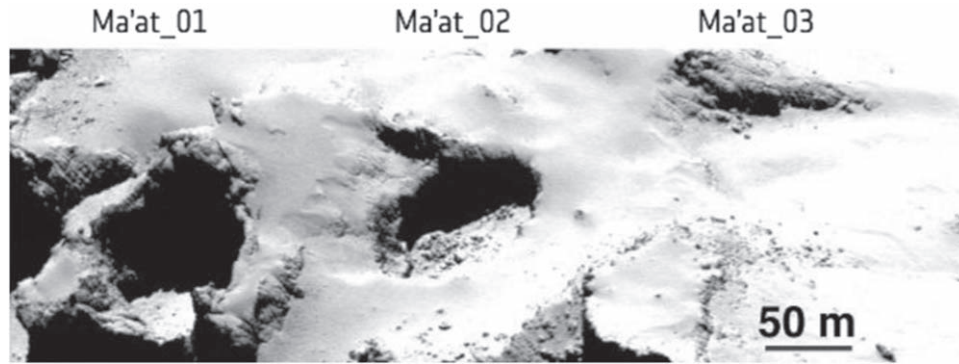


**Figure 1.** The evolution of cometary pits. The image was taken with the OSIRIS narrow-angle camera from a distance of 28 km from the surface of comet 67P. From left to right the pits measure 125 m, 130 m, and 140 m across and are 65 m, 60 m, and 50 m deep, respectively. Copyright: ESA/Rosetta/MPS for OSIRIS Team MPS/UPD/LAM/IAA/SSO/INTA/UPM/DASP/IDA.

## 2. Observational Studies of Comets

Observations are essential for the study of comets. We can distinguish the following methods:

1. ground telescopic observations,
2. the use of space telescopes (e.g., the Hubble telescope),
3. by sending space probes (e.g., Giotto, Stardust, Deep Impact and Rosetta).

In this paper, we assume that comet particles are composed of either ice and dust or of their interconnection. For this reason, testing the properties of the dust is crucial. In this context, the results of the Stardust space mission deserve special attention. The main target of this mission was Comet 81P/Wild, which was not selected by chance. Previously, this comet had a large circular orbit, but in September 1974 it came to just about 1 million km from Jupiter. The gravitational field of the gas giant changed its orbit and directed the comet toward the inner planets. In the time from the change of orbit to the flight of Stardust, the comet 81P/Wild approached the Sun five times. This means that the comet's chemical composition probably has not changed significantly since its inception. During the Stardust mission, dust samples were collected from the cometary tail and delivered to Earth in a probe capsule. The conducted research has shown that the dominant chemical element in the dust is magnesium (Engrand et al. 2016). Also, the presence of minerals associated with high temperatures was found.

It is worth noting that the recently completed mission Rosetta recorded many unique data related to the broadly understood activity of the comet 67P (Groussin et al. 2015; Preusker et al. 2015, 2017; Sierks et al. 2015; Tubiana et al. 2015; Lhotka et al. 2016; Marschall et al. 2016; Pätzold et al. 2016; Reimond & Baur 2016; Vincent et al. 2016a, 2016b). Let us recall that the primary goal of this mission was to enter orbit around comet 67P and place the Philae lander on its surface.

This mission, therefore, became a unique opportunity to trace the behavior of this object when it was most active. Rosetta performed in situ studies of cometary matter and made detailed observations of the surface of comet 67P nucleus. Also, Rosetta achieved the following goals:

1. Measurement of dynamic properties and nucleus morphology.
2. Examination of the chemical, mineralogical and isotopic composition of volatile and solid substances in the nucleus.
3. Determination of physical properties and relationships between volatile and solid substances in the nucleus.
4. Observation of the development phases of cometary activity and the processes taking place in the surface layer of the nucleus and the interactions between gas and dust.
5. Dynamic characterization and study of the chemical composition of the asteroids 21 Lutetia and 2867 Steins were performed.

At this point, it is worth noting that the results of the Rosetta mission indicated the possibility of different morphologies of cometary outbursts. At that time, several dozen outbursts of comet 67P were observed (Vincent et al. 2016a; Gicquel et al. 2017). They were caused by the emissions of matter from its nucleus in the form of jets (Vincent et al. 2016b). Let us add that the strongly collimated jets of gas and dust produced by cometary geysers were reported and studied theoretically for the comets 1P/Halley, 19P/Borrelly and 103P/Hartley (Keller 1990; Yelle et al. 2004; Belton 2010; A'Hearn et al. 2011; Gronkowski & Wesołowski 2015b, 2017).

Taking into account the above facts, we can conclude that cometary missions have provided us with a lot of information about comets and have also become an important tool complementing telescopic observations.

### 3. Evolution of Cometary Surface

Analyzing the results of the Rosetta mission, we can see that on the surface of comet 67P there are numerous pits, depressions and also cliffs. In most cases, the cometary activity was dominated by jets of gas and dust ejected from the nucleus. These active areas most likely arose as a result of a fracture or collapse of a fragment of the cometary surface (Vincent et al. 2016a, 2016b; Pajola et al. 2017). The direct cause is commonly believed to be the complex thermodynamic processes that take place inside the nucleus. In the case of comet 67P, such pits were observed at various locations on the surface of the nucleus. The location of the pits to which the occurrence of jets is attributed concerns the Seth and Ma'at areas (Vincent et al. 2015). Eighteen quasi-circular pits in the comet's northern hemisphere have been identified for the Seth region, some of which are a source of continued activity (Vincent et al. 2015). Whereas, for the Ma'at area, we can assign three main pits: Ma'at 1, Ma'at 2 and Ma'at 3 (see Figure 1).

These pits can be divided into two groups: active pits, i.e., young ones, and inactive pits, i.e., old ones. Note that the pits that are still active (e.g., Ma'at 1 and Ma'at 2) are steeper and deeper. In the case of inactive pits (Ma'at 3), over time, they can become filled with cometary material (e.g., dust agglomerates). Such filling of the cometary pit may be caused by dust migration on the nucleus surface (Wesołowski et al. 2019; Wesołowski 2020a) and by cometary avalanches (Wesołowski et al. 2020c). Let us add that both the migration of dust and avalanches were confirmed for comets 67P and 103P/Hartley (A'Hearn et al. 2011; Steckloff et al. 2015; Grün et al. 2016; Steckloff & Melosh 2016; Vincent et al. 2016a, 2016b; Pajola et al. 2017). In the context of studying the evolution of pits and cavities, the process of their formation is of key importance. In this case, we can discuss at least three typical processes. First, pits and cavities may be a relic of the time when the solar system and comets were formed. Second, the comet nucleus in its structure contains various types of ices that differ in their sublimation rates. This is especially true for those ices with low evaporation temperatures (CO, CO<sub>2</sub>), and this directly leads to sublimation from deeper layers of the cometary nucleus. Third, cometary nuclei in the early stages of their existence participated in collisions between small bodies then orbiting the Sun. To summarize, we can say that comet nuclei have an extremely interesting morphology. The development of a given model should include a "compromise." This mainly concerns the comet's chemical composition, its size and the fraction of the comet nucleus area that is active during the silent sublimation phase and the outburst phase. It should be clearly emphasized once again that in this respect every comet is different. Based on extensive observation material, we can

build a comet model that will try to reflect the real structure of the cometary nucleus.

### 4. Physical Model of the Cometary Outburst Phenomenon

The outburst of comets is related to the increase in brightness, i.e., more effective scatters of the incident light on the dust particles. The key challenge is to develop a model that leads to the local destruction of a comet nucleus fragment. Various mechanisms may be responsible for this destruction. Two mechanisms can be mentioned examples:

1. the pressure increase in the subsurface layers of the cometary nucleus,
2. intense sublimation of ice (H<sub>2</sub>O or CO<sub>2</sub>), which leads to the loosening of the dust layer on the nucleus surface.

As a result of this destruction and sublimation, these particles are emitted into the coma. This leads to an increase in the area on which the incident light scatters.

When developing a model of the thermodynamic evolution of the cometary nucleus, we use the equations of energy balance and sublimation rate, which were presented in detail in the paper Wesołowski (2021d, with references included therein). In the context of the sublimation rate, it should be noted that the classic Hertz–Knudsen formula should be corrected for the sublimation coefficient ( $\alpha_s(T)$ ) which determines the actual rate of sublimation through the cometary mantle (Kossacki et al. 1999, 2020).

Based on the model presented briefly, we can determine the thermodynamic parameters on the surface of the cometary nucleus. These parameters were used to determine the amplitude of the change in cometary brightness based on Pogson's law (Gronkowski et al. 2018; Wesołowski 2019, 2020d; Wesołowski et al. 2019, 2020b, 2020c). However, in this paper we will use an expanded form of Pogson's law

$$\Delta m = -2.5 \log \frac{p(\theta)_N C_N + p(\theta)_{\text{dust}}(C(t_2) + C(M_{\text{ej,dust}}))}{p(\theta)_N C_N + p(\theta)_{\text{dust}} C(t_1)}. \quad (1)$$

Note that Equation (1) was expressed by individual scattering cross-sections coming:

1. from the cometary nucleus ( $C_N$ );
2. from particles that were ejected to a coma during the quiet sublimation phase ( $C(t_1)$ ) and during the outburst ( $C(t_2)$ );
3. from the fragment of the cometary nucleus that has been destroyed ( $C(M_{\text{ej,dust}})$ ) during the outburst.

The individual cross-sections can be defined as:

$$C_N = A_N \cdot S_N, \quad (2)$$

**Table 1**  
Values of the Most Important Parameters that were Used in Numerical Simulations

Parameter	Value(s)	References
Radius of the comet nucleus (m)	$R_N = 2000$	Adopted value
Heliocentric distance (au)	$r = 1.5$	Adopted value
Density of cometary nucleus ( $\text{kg m}^{-3}$ )	$\rho_N = 400$	Richardson et al. (2007)
Density of cometary dust ( $\text{kg m}^{-3}$ )	$\rho_{\text{dust}} = 1200$	Calculated value
Albedo of cometary nucleus (...)	$A_N = 0.05$	Adopted value
Emissivity (...)	$\epsilon = 0.9$	Wesołowski et al. (2019)
Porosity (...)	$\psi = 0.6$	Adopted value
Radius of the coma (m)	$R_c(t_1) = 1 \times 10^8$	Wesołowski & Gronkowski (2018b)
Solar constant (for $d = 1$ au) ( $\text{W m}^{-2}$ )	$S_\odot = 1360.8 \pm 0.5$	Kopp & Lean (2011)
Constant $A_{\text{H}_2\text{O}}$ for water ice (Pa)	$A_{\text{H}_2\text{O}} = 3.56 \times 10^{12}$	Fanale & Salvail (1984)
Constant $B_{\text{H}_2\text{O}}$ for water ice (K)	$B_{\text{H}_2\text{O}} = 6141.667$	Fanale & Salvail (1984)
Latent heat of water ice sublimation ( $\text{J kg}^{-1}$ )	$L(T)_{\text{H}_2\text{O}} = 2.83 \times 10^6$	Adopted value
Constant $A_{\text{CO}_2}$ for carbon dioxide (Pa)	$A_{\text{CO}_2} = 107.9 \times 10^{10}$	Adopted value
Constant $B_{\text{CO}_2}$ for carbon dioxide (K)	$B_{\text{CO}_2} = 3148.0$	Adopted value
Latent heat of carbon dioxide sublimation ( $\text{J kg}^{-1}$ )	$L(T)_{\text{CO}_2} = 0.594 \times 10^6$	Adopted value
Wavelength of electromagnetic solar radiation (m)	$\lambda = 0.50 \times 10^{-6}$	Wesołowski et al. (2020b)
The average radius of the cometary agglomerate (m)	$r_{\text{agg}} = 14.2 \times 10^{-6}$	Wesołowski et al. (2020b)
The diameter of the pits (m)	$d_{\text{ej}} = 10; 30; 50; 70$	Adopted value
Refractive index for cometary dust (...)	$n_{\text{si}} = 1.60 + 0.005i$	Adopted value
The scattering factor for cometary dust particles (...)	$Q_{\text{agg}} = 1.173$	Calculated value

$$C(t_1) = \frac{3\pi\eta(t_1)\kappa R_N^2 \dot{Z}(\alpha_s(T)) R_c(t_1) m_g \int_{r_{\min}}^{r_{\max}} Q_{\text{scat}}(r, m^*, \lambda) r^2 f(r) dr}{v_g \rho_{\text{gr}} \int_{r_{\min}}^{r_{\max}} r^3 f(r) dr}, \quad (3)$$

$$C(t_2) = \frac{3\pi\eta(t_2)\kappa R_N^2 \dot{Z}(\alpha_s(T)) R_c(t_2) m_g \int_{r_{\min}}^{r_{\max}} Q_{\text{scat}}(r, m^*, \lambda) r^2 f(r) dr}{v_g \rho_{\text{gr}} \int_{r_{\min}}^{r_{\max}} r^3 f(r) dr}, \quad (4)$$

$$C(M_{\text{ej,dust}}) = \frac{3\pi d_{\text{ej}}^2 h \int_{r_{\min}}^{r_{\max}} Q_{\text{scat,dust}}(r, m^*, \lambda) r^2 f(r) dr}{16 \int_{r_{\min}}^{r_{\max}} r^3 f(r) dr}. \quad (5)$$

In Equations (1)–(5) the individual symbols mean:  $p(\theta)_N$ ,  $p(\theta)_{\text{dust}}$ ,  $p(\theta)_{\text{ice}}$  denote the value of the phase function for the cometary nucleus and the ice-dust particles, respectively. The other symbols mean:  $r$  is the radius of cometary particles,  $m^*$  is the complex effective refractive index of dust, and the value of the wavelength  $\lambda$  to be determined by the Wien law applied to the Sun's radiation,  $\kappa$ —the dust-gas mass ratio,  $S_N$  is the total area of the comets,  $R_N$  is its radius,  $R_c(t_i)$ —radius of the cometary coma in the quiet sublimation ( $t_1$ ) and outburst phase ( $t_2$ ),  $m_g$ —the mass of cometary gas,  $\rho_{\text{gr}}$ —the density of the dust particles,  $v_g$ —the mean radial velocity of gas molecules,  $d_{\text{ej}}$ —the diameter of the pits, and  $h$ —the depth of the cometary pit. The other symbols have the same meanings as above. Note

that  $Q_{\text{scat}}(r, m^*, \lambda)$  are the scattering efficiency of dust agglomerates. It should be noted that in the case of particles consisting of dust, the Discrete Dipole Approximation theory was used (see e.g.,: Zubko et al. 2011). However, to determine analogous characteristics for dust agglomerates, we rely on the results of appropriate calculations based on the theory of the discrete dipole approximation and presented by Zubko (2013). In individual scattering cross-sections (Equations (3)–(5)) we used the following distribution function for dust agglomerates (Lin et al. 2017)

$$f(r) = C \cdot r^{-3.7}, \quad (6)$$

where  $r$  and  $C$  are the radius of the effective cross-section of fluffy aggregate and the normalizing constant, respectively. The value of  $-3.7$  results from the adopted range of cometary particle sizes, which is from  $10^{-6}$  to  $10^{-3}$  m. Moreover, the value of this coefficient is consistent with the analysis by Fulle et al. (2016).

Note that in Equations (3)–(4) there are two important parameters:  $\eta(t_1)$  and  $\eta(t_2)$  which represent the fraction of the cometary nucleus surface that is active in the quiet sublimation phase and the outburst phase. Based on the analysis of many observational data obtained during space missions (Deep Impact, EPOXI), we were able to estimate the real value of the parameter  $\eta(t_1)$ . Typically, the value of this parameter is around 5% and should be considered a free parameter. In the case of comet 67P, as shown by Keller et al. (2017), the value of the  $\eta(t_1)$  parameter may be much higher.

When calculating the total active area during an outburst ( $\eta(t_2)$ ), two factors should be taken into account. The first is the surface that is active in the silent phase of sublimation ( $\eta(t_1)$ ), and the second is the ratio of the ejected area ( $S_{ej}$ ) to the total area of the comet nucleus ( $S_N$ ). In other words, the second part is an amendment related to the destruction of a fragment of the cometary nucleus. Based on the evolution of the pits, this amendment can be defined as

$$\Delta\eta = \frac{S_{ej}}{S_N} = \frac{d_{ej}^2}{16R_N^2}. \quad (7)$$

Then the total surface active during the cometary outburst is given by the relationship

$$\eta(t_2) = \eta(t_1) + \frac{d_{ej}^2}{16R_N^2}. \quad (8)$$

Then the following relation is fulfilled:  $\eta(t_2) > \eta(t_1)$ .

## 5. Results of Numerical Calculations

Numerical calculations were performed for the hypothetical comet X/JFC based on the model of the evolution of the surface and subsurface layers. The calculations assume that the cometary outburst took place at one of the three heliocentric distances of  $r_1 = 1.5$  au,  $r_2 = 3.0$  au or  $r_3 = 4.5$  au. The remaining parameters used in the numerical simulations are presented in Table 1. It was also assumed that the cometary activity was controlled by the sublimation of water ice and carbon dioxide that occurred from the interior of the cometary nucleus. Our considerations focus mainly on the study of the scattering of incident sunlight that occurs on dust agglomerates with porosity  $\psi = 0.6$ . In these calculations, the average value of the radius of porous dust agglomerates was adopted, determined based on the appropriate distribution functions (see Equation (6), and Appendix in Wesołowski et al. 2020b). In the context of the analysis of the change in the brightness of the comet, it should be noted that the key factor is the number of dust particles that are in the coma. The number of these particles is directly related to the total surface area of the comet nucleus that has been destroyed. Additionally, the number of particles can be increased by local sublimation of the cometary ice. As a result, particles with process dimensions of up to centimeters may be carried into the coma (see Gronkowski & Wesołowski 2015b, 2017). In this case, the key parameters are the rate of sublimation, particle density and the radius of the cometary nucleus (Wesołowski et al. 2020a). The results of numerical simulations related to the cometary outburst are presented in Figures 2–7.

## 6. Summary and Discussion

This paper presents an analysis of cometary cavities based on the mechanism of the thermodynamic evolution of the sinkhole

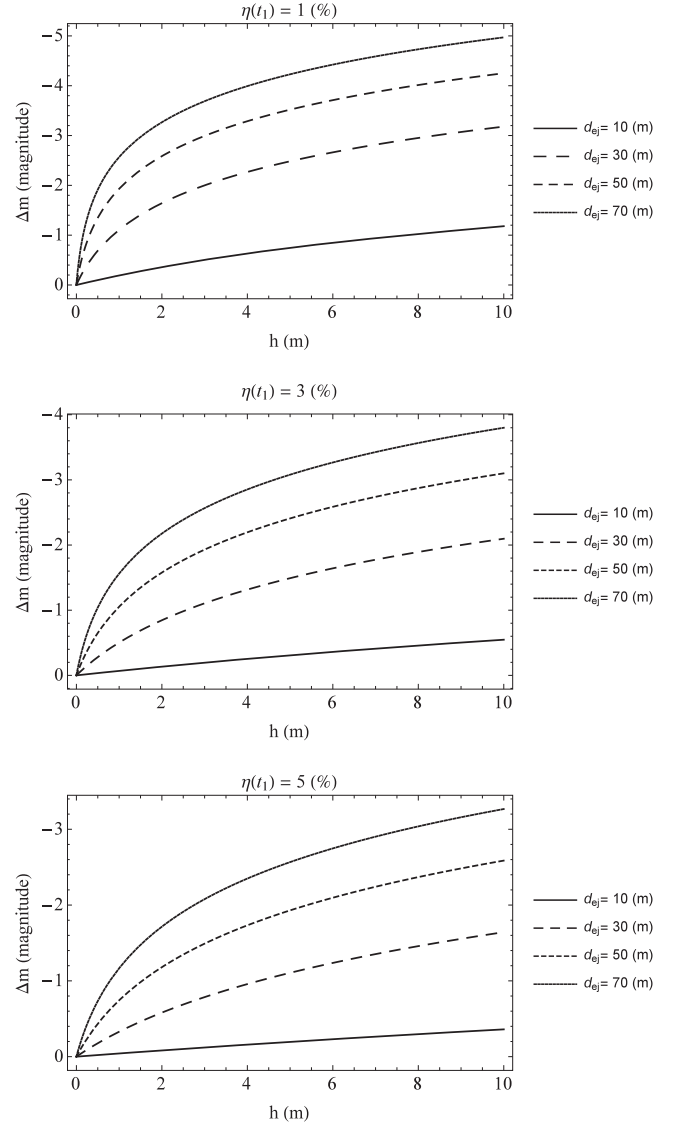


**Figure 2.** The brightness jump  $\Delta m$  for a comet during its outbursts as a function of depth and diameter of the pit. Furthermore, cometary activity is assumed to be controlled by the sublimation of water ice, occurring from the interior of the nucleus. The scattering of the incident sunlight concentrates on the porous dust agglomerates. The calculations assume that the comet is at a heliocentric distance of  $r_1 = 1.5$  au. Additionally, it was assumed that the  $\eta(t_1)$  parameter was equal to 1%, 3% and 5%, from the top panel to bottom panel respectively.

(pit). The performed calculations focused on determining the change in the cometary brightness as a result of the resulting sinkhole. The measure of this brightness is the fraction of the area and thickness of the destroyed cometary nucleus layer. Note that these two parameters determine the total mass ejected during the outburst. It is worth noting that the amplitude of the brightness of the comet presented above represents the maximum values. This means that in the simulation of the

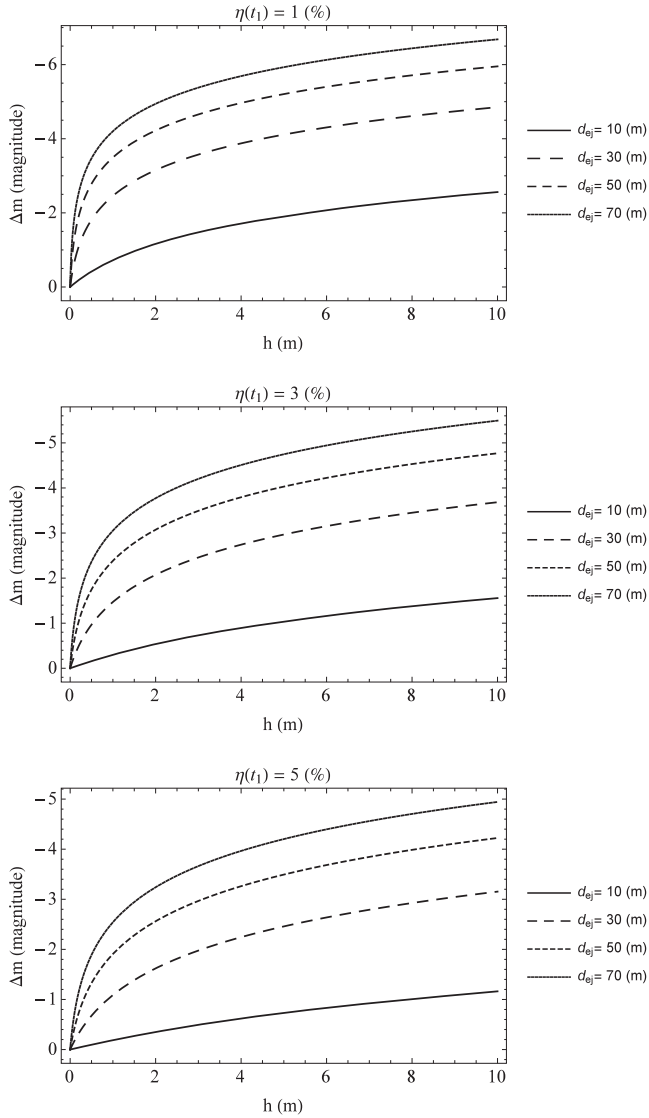


**Figure 3.** Similar to Figure 2, but calculations assume that the cometary outburst occurred at a heliocentric distance  $r_1 = 3.0$  au.

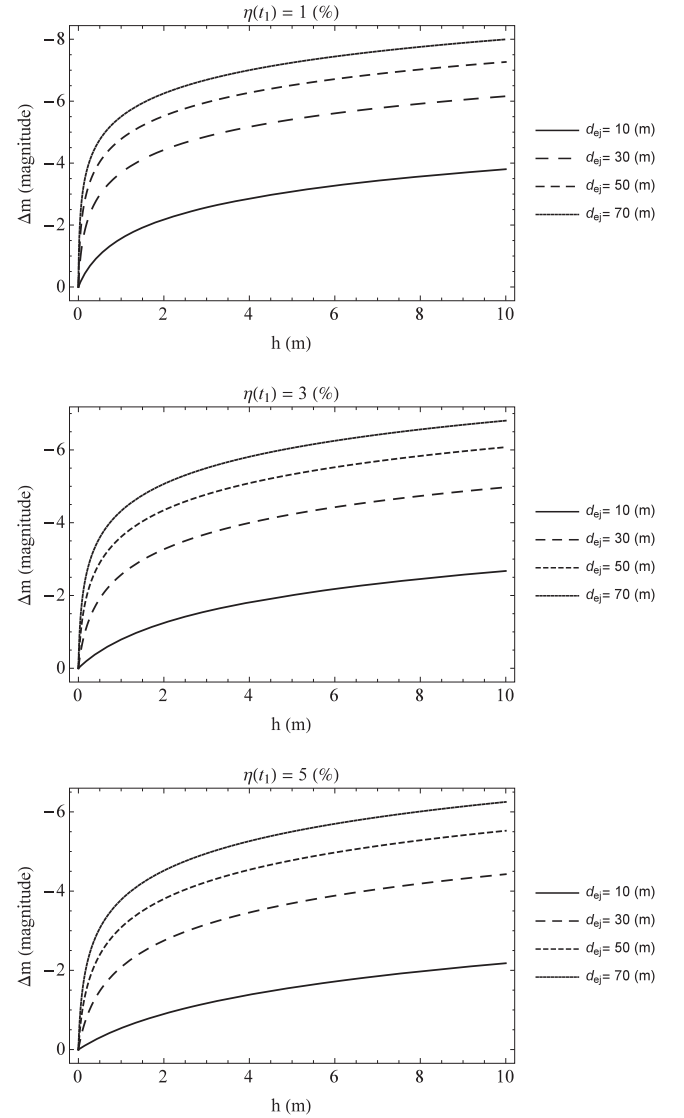


**Figure 4.** Similar to Figure 2, but calculations assume that the cometary outburst occurred at a heliocentric distance  $r_1 = 4.5$  au.

outburst, the maximum value of the mass ejected related to a given sinkhole was taken into account. Thus, the formation of a sinkhole may be a sudden process related to the voids of cavities in the comet nucleus. Such spaces as a result of the sublimation of  $\text{CO}_2$  ice and  $\text{CO}$  ice that occurs from inside the nucleus evolve over time. As a consequence, the upper layer may become unstable, which eventually collapses (Sierks et al. 2015). As a consequence, there is an increase in the amount of dust particles in the coma, which translates into the effectiveness of scattering the incident sunlight. Then we can observe the cometary outburst.

The dimensions of a given excavation may increase in much longer timescales due to the erosion of the surface and

subsurface layers. As mentioned above, pits can be divided into two types. In the case of active ones, gas streams coming from the inner walls of an active pit are visible. There are also visible cracks on the walls inside the excavation (Vincent et al. 2015). Thanks to the existence of the pits and the use of the results of the Rosetta mission, we can almost look inside the cometary nucleus. The process of evolution of the pits allows us to study the original comet material, which under typical conditions is unavailable to us. From the number of active pits on the surface of the nucleus, we can estimate the comet's relative age. This means how long the comet remains in the inner solar system. It seems that the number of pits, especially the young (active)

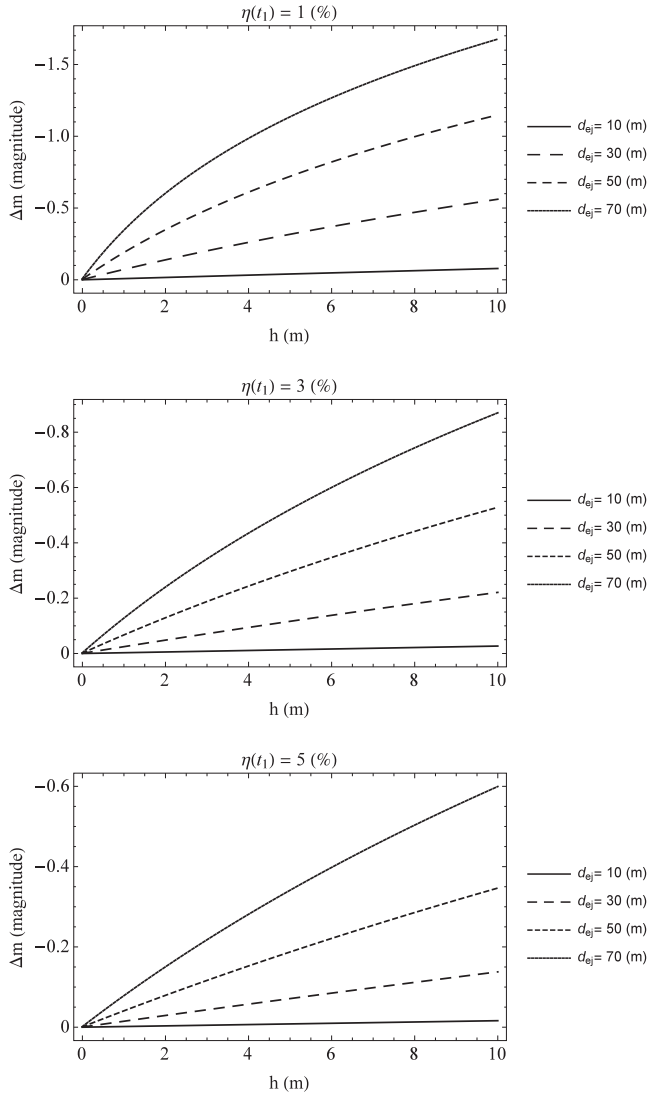


**Figure 5.** Similar to Figure 2, but calculations assume that cometary activity is controlled by carbon dioxide sublimation.

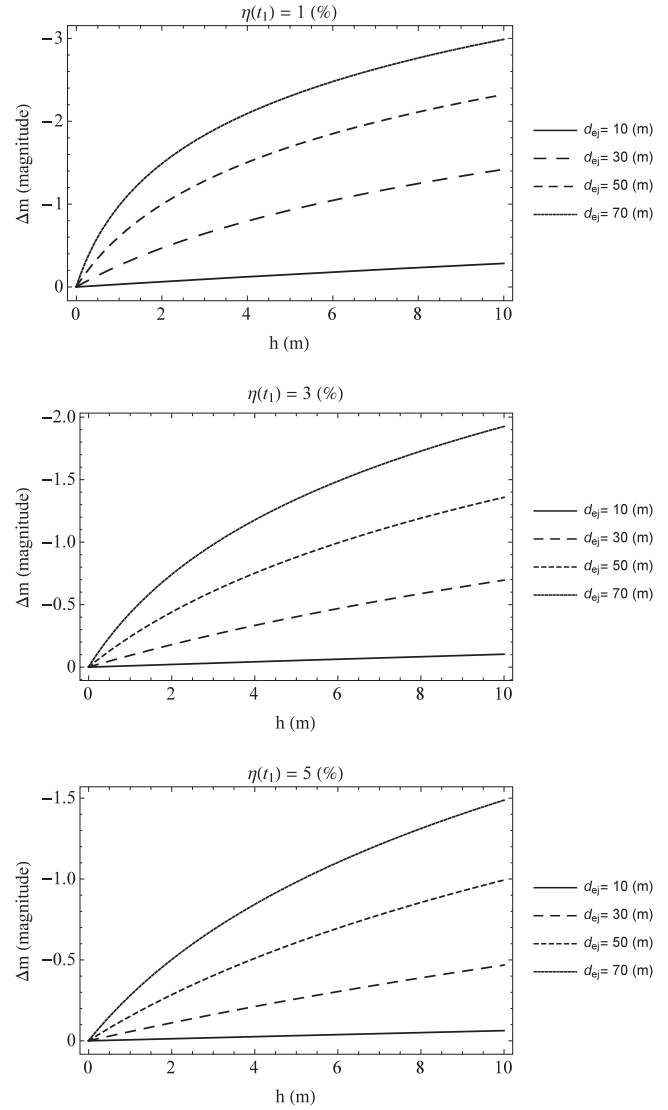


**Figure 6.** Similar to Figure 3, but calculations assume that cometary activity is controlled by carbon dioxide sublimation.

ones, indicates a less processed area of the cometary nucleus (Vincent et al. 2015).

Moreover, the simulations show that:

1. The calculated values of the comet brightness change are correct for comets whose spectrum is continuous.
2. The cometary outbursts last from a few to several days. This is a very short time compared to the comet's orbital period, so its phase angle changes very little.
3. The cometary brightness jump depends on the value of  $\eta(t_1)$  parameters—the lower the value of this parameter, the greater the cometary brightness jump (Wesołowski & Gronkowski 2018a, 2018b, Wesołowski et al. 2020b, 2020c; Wesołowski 2020c, 2022).
4. Due to the dimensions of the pits and cavities, quiet sublimation cannot be a process responsible for the formation of such structures, even on a longer timescale. This statement applies to relatively young comets, i.e., those that orbit relatively shortly in the inner solar system (e.g., 67P).
5. However, in the long term, at least the shape of the upper of the pit may change. The process is related to sublimation from the exposed inner walls of the pit, which are illuminated by the Sun. However, this process requires further research, if only because of the shading of a fragment of the walls of a given pit.
6. The most likely cause of pits is the formation of a sinkhole, e.g., collapse of the material into cavities.

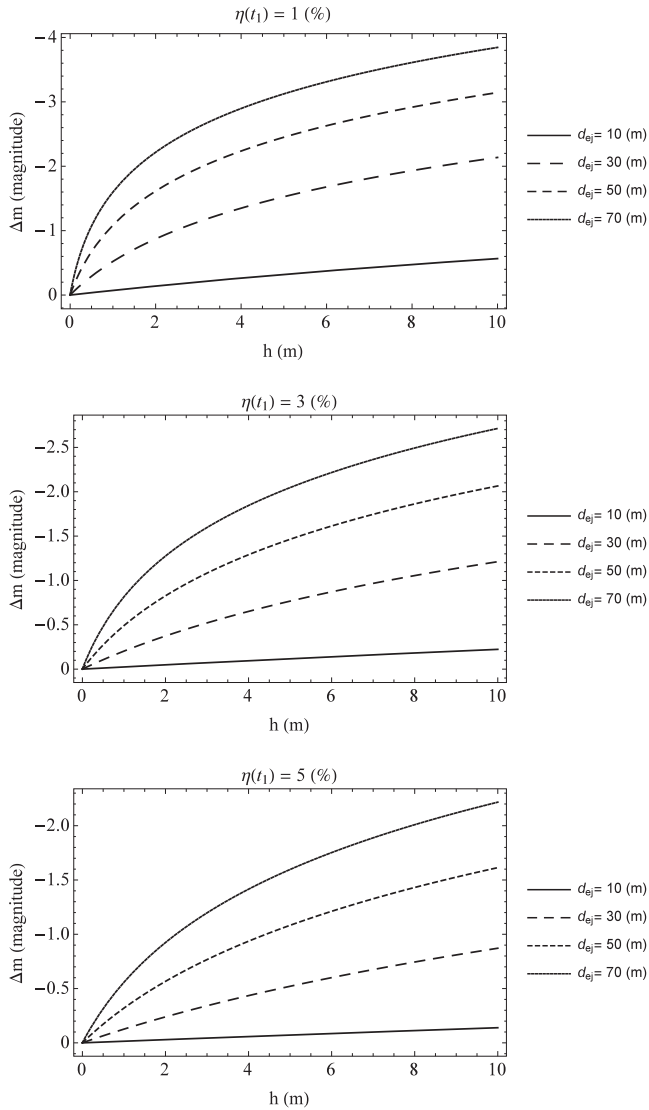


**Figure 7.** Similar to Figure 4, but calculations assume that cometary activity is controlled by carbon dioxide sublimation.

By analyzing the obtained numerical values of the change in the brightness of a comet during its outburst, conclusions can be drawn. In the case of cometary activity controlled by sublimation of water ice, the amplitude of the change in brightness ranges from  $-1.5$  to about  $-7$  mag. However, in the case of carbon dioxide controlled sublimation, the amplitude ranges from  $-0.1$  to about  $-4.0$  mag. Note that these differences relate to the maximum values. This difference is a consequence of the considered thermodynamic model which is represented by two basic parameters such as the sublimation rate and the velocity of the gas molecules. Also, the differences depend on the size of the  $\eta(t_1)$  parameter, the diameter of the pits  $d_{ej}$  as well as the size of the cometary nucleus and the

heliocentric distance at which the outburst took place. It should be emphasized once again that the measure of the change in brightness is the amount of dust in the coma. This value is determined by knowing the depth and diameter of the pit from which matter was ejected into space by the jet. It is worth noting that the obtained variations in comet brightness are consistent with actual comet outbursts, which have been discussed at length in the Introduction of this paper.

In addition, a simulation was performed for the actual outburst of comet 67P, which took place in 2014 at a distance of 4.1 au. From these considerations, it follows that with the increase of the surface that was active during the quiet sublimation, the diameter of the pit increases for the same change in the brightness of the comet. Of course, this result was not surprising, but it reflected many years of comet observations.

The presence of pits and cavities in the comet structure appears to be a typical comet morphology, especially for the Jupiter family of comets. This is confirmed by the observations of comets 9P/Tempel (Deep Impact), 81P/Wild (Stardust) and 67P/Churyumov–Gerasimenko (Rosetta), during which similar structures to pits and cavities were observed. Let us emphasize that by researching these structures we can follow the evolution of these celestial bodies.

### Acknowledgments

This work has been done due to the support the author received from the Centre for Innovation and Transfer of Natural Sciences and Engineering Knowledge, University of Rzeszów, Poland.

### Appendix The Outburst of Comet 67P/Churyumov–Gerasimenko

Based on the model presented in the main part of the paper, a numerical simulation of the outburst of comet 67P, which took place at the end of April 2014, was carried out. This outburst occurred several months before the comet reached its perihelion. The Rosetta devices recorded a sudden increase in the brightness of the comet from 17.2 to 16.6 mag at a distance of  $d = 4.1$  au. This corresponds to a change in the cometary brightness by  $\Delta m = -0.6$  mag. In these calculations, it was assumed that the activity of comet 67P was controlled by the sublimation of  $\text{CO}_2$  ice. On this basis, the mass flow rate and the fraction of the area that was active during this outburst were determined. Subsequently, the diameter of the pit was determined, which was related to its constant depth and the fraction of the area that was active during this outburst. When analyzing the outburst activity of comet 67P, it should be stated that the amplitude of the change in brightness during most of the outbursts oscillated around 1 mag. The probable cause of such a low change in brightness value may be a relatively large

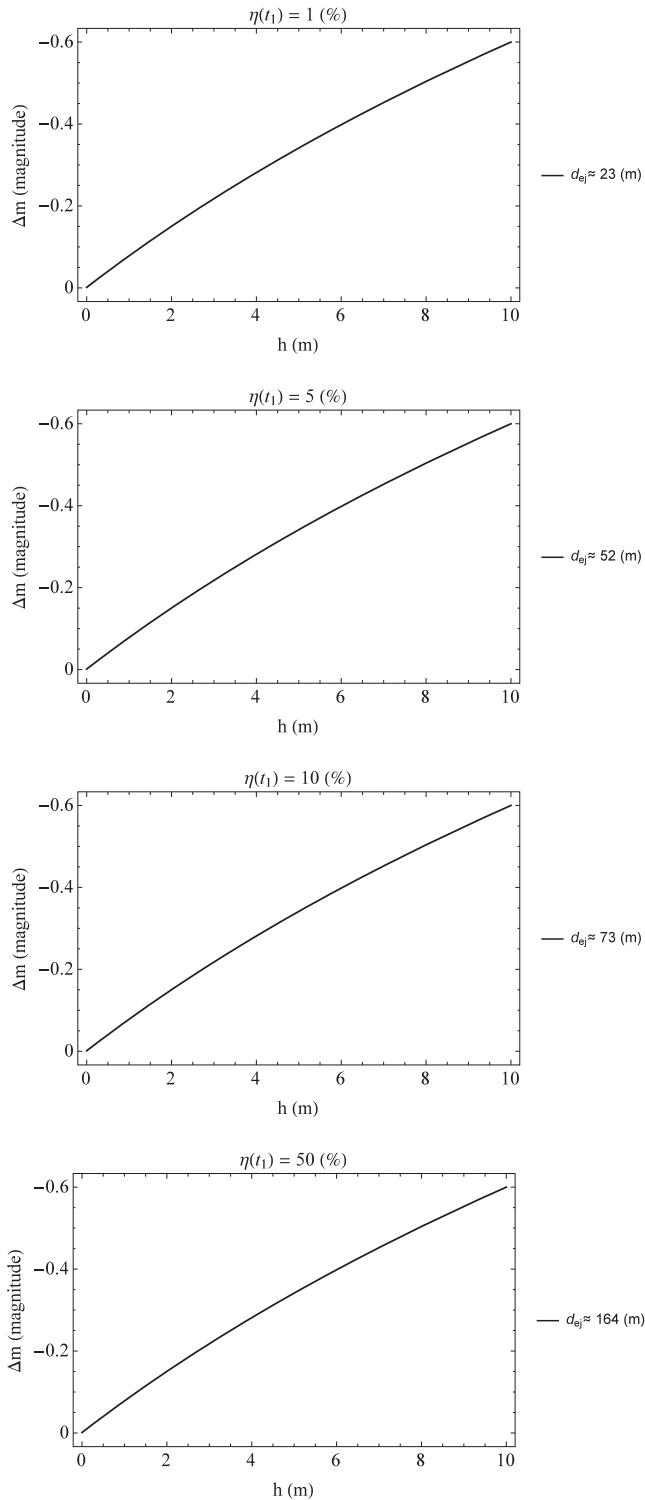


**Figure A1.** Change in the brightness of comet 67P during its outburst in 2014.

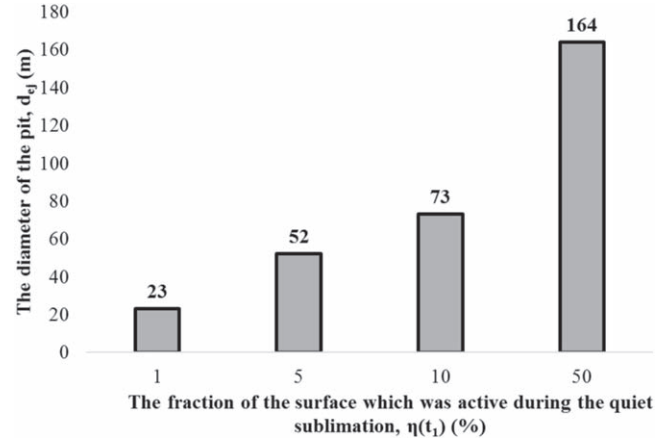


**Figure A2.** The distribution of the pit diameter as a function of the area fraction that was active during quiet sublimation. The presented calculations are for comet 67P for which the change in brightness was  $\Delta m = -0.6$  mag (see Figure A1).

percentage of the surface that was active during the quiet sublimation and during the outburst. The result of these calculations is presented in Figures A1–A2.

### ORCID iDs

Marcin Wesołowski  <https://orcid.org/0000-0002-5049-4323>

### References

- A’Hearn, M. F., Belton, M. J. S., Delamere, W. A., et al. 2011, *Sci*, **332**, 1396  
 Belton, M. J. S. 2010, *Icar*, **210**, 881  
 Cabot, H., Enzian, A., Klinger, J., & Majolet, S. 1996, *P&SS*, **44**, 1015  
 Engrand, C., Duprat, J., Dartois, E., et al. 2016, *MNRAS*, **462**, 323  
 Enzian, A., Cabot, H., & Klinger, J. 1997, *A&A*, **319**, 995  
 Fanale, F. P., & Salvail, J. R. 1984, *Icar*, **60**, 476  
 Fulle, M., Marzari, F., Della Corte, V., et al. 2016, *ApJ*, **821**, 19  
 Gicquel, A., Rose, M., Vincent, J.-B., et al. 2017, *MNRAS*, **469**, 178  
 Gronkowski, P., Tralle, I., & Wesołowski, M. 2018, *AN*, **339**, 37  
 Gronkowski, P., & Wesołowski, M. 2012, *AN*, **333**, 721  
 Gronkowski, P., & Wesołowski, M. 2015a, *MNRAS*, **451**, 3068  
 Gronkowski, P., & Wesołowski, M. 2015b, *AN*, **336**, 362  
 Gronkowski, P., & Wesołowski, M. 2016, *EM&P*, **119**, 23  
 Gronkowski, P., & Wesołowski, M. 2017, *AN*, **338**, 385  
 Groussin, O., Jorda, L., Auger, A.-T., et al. 2015, *A&A*, **583**, A32  
 Grün, E., Agarwal, J., Altobelli, N., et al. 2016, *MNRAS*, **462**, 220  
 Güttler, C., Mannel, T., Rotundi, A., et al. 2019, *A&A*, **630**, A24  
 Ivanova, O. V., Skorov, Y. V., Korsun, P. P., et al. 2011, *Icar*, **211**, 559  
 Keller, H. U. 1990, *The Nucleus* (Berlin: Springer), 21  
 Keller, H. U., & Kührt, E. 2020, *SSRv*, **216**, 14  
 Keller, H. U., Mottola, S., Hviid, S. F., et al. 2017, *MNRAS*, **469**, 357  
 Kopp, G., & Lean, J. L. 2011, *GeoRL*, **38**, L01706  
 Kossacki, K. J., Markiewicz, W. J., Skorov, Y., et al. 1999, *P&SS*, **47**, 1521  
 Kossacki, K. J., Skóra, G., & Czechowski, L. 2020, *Icar*, **348**, 113781

- Lhotka, C., Reimond, S., Souchay, J., et al. 2016, *MNRAS*, 455, 3588
- Lin, Z.-Y., Knollenberg, J., Vincent, J.-B., et al. 2017, *MNRAS*, 469, 731
- Marschall, R., Su, C. C., Liao, Y., et al. 2016, *A&A*, 589, A90
- Miles, R. 2016, *Icar*, 272, 356
- Pajola, M., Höfner, S., Vincent, J.-B., et al. 2017, *NatAs*, 1, 92
- Pätzold, M., Andert, T., Hahn, M., et al. 2016, *Nat*, 530, 63
- Preusker, F., Scholten, F., Matz, K.-D., et al. 2015, *A&A*, 583, A33
- Preusker, F., Scholten, F., Matz, K.-D., et al. 2017, *A&A*, 607, 1
- Reimond, S., & Baur, O. 2016, *JGRE*, 121, 497
- Richardson, J. E., Melosh, H. J., Lisse, C. M., et al. 2007, *Icar*, 190, 357
- Sierks, H., Barbieri, C., Lamy, P. L., et al. 2015, American Geophysical Union, P33E-02
- Steckloff, J., Graves, K., Hirabayashi, M., et al. 2015, DPS Meeting, 47, 415.06
- Steckloff, J., & Melosh, H. J. 2016, DPS Meeting, 48, 206.06
- Tubiana, C., Snodgrass, C., Bertini, I., et al. 2015, *A&A*, 573, A62
- Vincent, J. B., A'Hearn, M. F., Lin, Z.-Y., et al. 2016a, *MNRAS*, 462, 184
- Vincent, J. B., Bodewits, D., Besse, S., et al. 2015, *Nat*, 523, 63
- Vincent, J.-B., Oklay, N., Pajola, M., et al. 2016b, *A&A*, 587, A14
- Wesołowski, M. 2019, *JApA*, 40, 20
- Wesołowski, M. 2020a, *JApA*, 41, 1
- Wesołowski, M. 2020b, *RAA*, 20, 132
- Wesołowski, M. 2020c, *Icar*, 351, 113950
- Wesołowski, M. 2020d, *P&SS*, 194, 105117
- Wesołowski, M. 2021a, *Icar*, 357, 114116
- Wesołowski, M. 2021b, *RAA*, 21, 69
- Wesołowski, M. 2021c, *NewA*, 89, 101626
- Wesołowski, M. 2021d, *MNRAS*, 505, 3525
- Wesołowski, M. 2022, *Icar*, 375, 114847
- Wesołowski, M., & Gronkowski, P. 2018a, *NewAst*, 62, 55
- Wesołowski, M., & Gronkowski, P. 2018b, *EM&P*, 121, 105
- Wesołowski, M., Gronkowski, P., & Tralle, I. 2019, *MNRAS*, 484, 2309
- Wesołowski, M., Gronkowski, P., & Tralle, I. 2020a, *Icar*, 338, 113546
- Wesołowski, M., Gronkowski, P., & Tralle, I. 2020b, *P&SS*, 184, 104867
- Wesołowski, M., Gronkowski, P., & Tralle, I. 2020c, *Icar*, 352, 114005
- Yelle, R. V., Soderblom, L. A., & Jokipii, J. R. 2004, *Icar*, 167, 30
- Zubko, E. 2013, *EP&S*, 65, 13
- Zubko, E., Furusho, R., Kawabata, K., et al. 2011, *JQSRT*, 112, 1848